PRESSURE WAVES IN MICROSCOPIC SIMULATIONS OF LASER ABLATION

LEONID V. ZHIGILEI and BARBARA J. GARRISON

Department of Chemistry, The Pennsylvania State University, University Park, PA 16802

ABSTRACT

Laser ablation of organic solids is a complex collective phenomenon that includes processes occurring at different length and time scales. A mesoscopic breathing sphere model developed recently for molecular dynamics simulation of laser ablation and damage of organic solids has significantly expanded the length-scale (up to hundreds of nanometers) and the time-scale (up to nanoseconds) of the simulations. The laser induced buildup of a high pressure within the absorbing volume and generation of the pressure waves propagating from the absorption region poses an additional challenge for molecular-level simulation. A new dynamic boundary condition is developed to minimize the effects of the reflection of the wave from the boundary of the computational cell. The boundary condition accounts for the laser induced pressure wave propagation as well as the direct laser energy deposition in the boundary region.

INTRODUCTION

Traditional computational material modeling methods are based either on macroscopic continuum-mechanics theories or atomistic simulation techniques. Recently, substantial progress has been made in development of advanced multiscale simulation techniques aimed at bridging the gap between the atomistic and continuum descriptions.[1,2,3,4,5] These techniques include a direct combination of atomistic and continuum finite element methods to simulate an adequate response of surrounding material to the active localized processes in the atomistic computational cell[2,3,4] and multiscale hierarchic approaches, in which accurate atomic-scale calculations provide data for parametrization of macroscopic or mesoscopic models.[1,5] These techniques, however, are hardly applicable for systems in which the critical events are not localized and the processes occurring at different length scales are inherently coupled and should be considered simultaneously.

An example of such a complex multiscale phenomenon considered in this work is laser ablation of an organic solid.[6] The processes involved in laser ablation include laser excitation of absorbing molecules, energy transfer from the excited molecules into the internal and translational modes of other molecules in the solid, formation of a highly energetic high-temperature and high-pressure region, explosive disintegration and prompt forward ejection of a volume of material, intensive processes in the ejected plume, and propagation of the pressure wave away from the ablation region. The complex character of the involved intertwined processes hinders an adequate analytical formulation for a continuum description of the phenomenon whereas a collective character of the laser ablation occurring at the mesoscopic rather than molecular scale does not permit a direct application of the atomistic simulation approach. An alternative mesoscopic model that has advantage of both addressing the effects of laser irradiation at a submicron resolution and yet incorporating a realistic description of energy relaxation of individual molecules internally excited by photon absorption has been developed recently for molecular dynamics (MD) simulation of laser ablation and damage of organic solids.[7]

In this paper we shortly review the basic features of the model, give a few examples of simulation setups used to study the laser induced processes in practically important applications, and focus on the computational approach used to deal with the laser induced pressure waves.

Mat. Res. Soc. Symp. Proc. Vol. 538 © 1999 Materials Research Society

THE BREATHING SPHERE MODEL

In this section we give only a brief description of the breathing sphere model for molecular dynamics simulations of laser ablation and damage in organic solids. Complete details of the model are given in Ref. 7.

The model assumes that each molecule (or appropriate group of atoms) can be represented by a single particle that has the true translational degrees of freedom but an approximate internal degree of freedom. The internal degree of freedom is attributed to each molecule by allowing the particles to change their sizes. The characteristic frequency of the internal motion, Fig. 1, is controlled by the parameters of an anharmonic potential. The rate of the intermode energy transfer is determined by the size of the anharmonicity and frequency mismatch between vibrational modes. Thus, the parameters of the internal potential can be used to affect the coupling between internal and translational molecular motions and to achieve a desired rate of the conversion of internal energy of the molecules excited by the laser to the translational and internal motion of the other molecules.

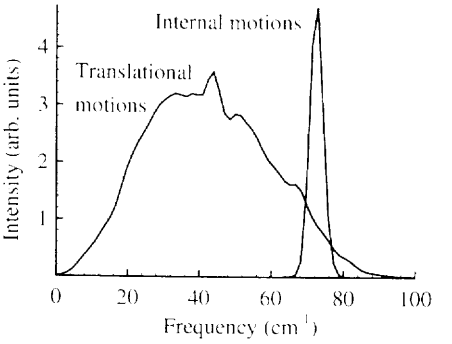

Figure 1. Vibrational spectrum of the breathing sphere model at 300 K. The coupling between internal and translational motions defines the rate of the vibrational relaxation of excited molecules.

Because the molecules and not the atoms are the particles of interest, the system size can be significantly larger. Moreover, since explicit atomic vibrations are not followed, the timestep in the numerical integration is longer. One more advantage of the breathing sphere model is the ability to simulate complex multicomponent organic materials. We can easily include bonding interactions, different strengths and absorptions of different components. The rate of energy transfer within an individual component as well as between components can be precisely controlled.

The effect of laser irradiation is simulated by vibrational excitation of random molecules during the time of the laser pulse within the penetration depth appropriate for a given wavelength. Vibrational excitation is modeled by depositing a quantum of energy equal to the photon energy into the kinetic energy of internal vibration of a given molecule. The absorption

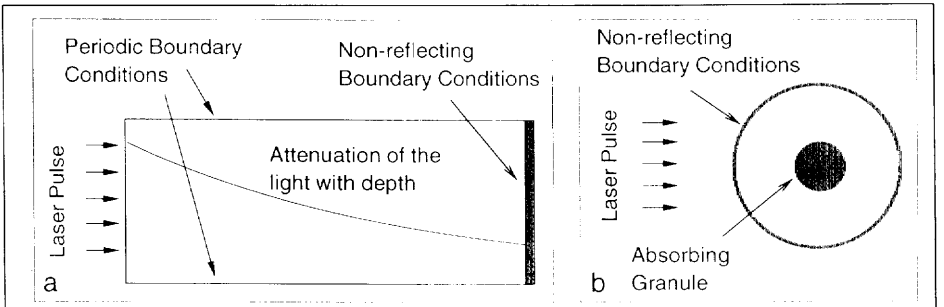

Figure 2. Schematic sketches of the simulation setups used in the simulations.

probability can be modulated by Beer's law to reproduce the exponential attenuation of the laser light with depth or can be restricted to a certain component within a complex material.

Two simulation setups that have been used to study the laser induced processes are shown in Fig. 2. Simulations performed with a setup shown in Fig. 2a are used to study the basic microscopic mechanisms of laser ablation,[7,8] and have yielded predictions on the threshold behavior,[8,9] composition of the ejected plume[7,8,9] and velocity distributions of ejected molecules.[10] The computational setup used to investigate mechanisms of laser damage in the case of spatially localized absorbers (absorbing particles embedded in a transparent medium)[11] is shown in Fig. 2b.

Owing to the approximations adopted in the breathing sphere model, computational cells schematically shown in Fig. 2 can be large enough to reproduce the collective dynamics leading to laser ablation and damage. One effect, however, that can not be directly simulated within the MD model is propagation of the laser induced elastic wave. The origin of the wave and the method used to minimize the effects of the reflection of the wave from the boundary of the computational cell are discussed in the next section.

PRESSURE WAVES AND NON-REFLECTING BOUNDARY CONDITION

The role of the laser induced pressure and associated photomechanical effects in laser ablation is defined by the irradiation parameters.[12,13] When the laser pulse width is shorter than a characteristic time of mechanical relaxation, the laser heating takes place at nearly constant volume conditions and leads to a high thermoelastic pressure buildup within the absorbing volume. For longer laser pulses the laser heating is more gradual, the material has sufficient time to expand during the laser pulse, and material removal is induced by thermal evaporation occurring under ambient pressure.

It is the former case of the short pulse irradiation that poses an additional challenge for molecular-level simulations. The laser induced pressure leads to the formation of the pressure wave that propagates in all directions from the absorption region. Propagation of the stress wave occurs at the length-scales that are beyond the capability of the breathing sphere model. This is illustrated in Fig. 3 where the formation and propagation of a plane pressure wave within the MD computational cell is given for the simulation setup shown in Fig. 2a. Even for a large, 180 nm in the direction of the wave propagation, computational cell, the pressure wave reaches the boundary of the simulation zone in less than 70 ps. This time is significantly shorter than the

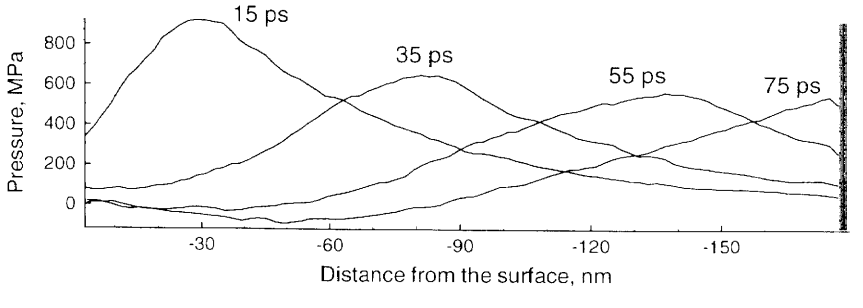

Figure 3. Formation and propagation of the pressure wave for the computational setup shown in Fig. 2a. Laser fluence is 55 J/m^2, penetration depth is 50 nm, and pulse width is 15 ps. Non-reflecting boundary condition applied at the depth of 180 nm is described in the text below.

characteristic time of the processes involved in laser ablation and artificial border effects can interfere with the simulation results. Both rigid and free boundary conditions lead to the complete reflection of the pressure wave and can cause fracturing at a certain depth when the tensile strength is exceeded. Such process of a subsurface fracture is termed spallation and is illustrated in Fig. 4. In this simulation spallation at the back side of the irradiated sample is caused by reflection of the unloading wave propagating from the surface of the irradiated sample. The laser penetration depth in this case is longer than the size of the computational cell leading to nearly even initial energy and pressure distributions within the sample. Interestingly, the spallation at the back is observed at a laser fluence about half of the threshold fluence for the onset of the massive material ejection or ablation[8,9] at the front surface.

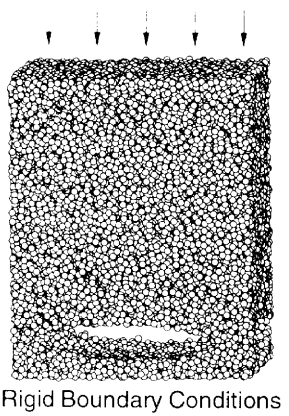

Figure 4. Back spallation due to interaction of the laser induced pressure wave with a rigid boundary of the computational cell.

Several approaches can be used to minimize the finite size artifacts and simulate the non-reflecting propagation of the stress wave out from the MD computational cell. A number of "reservoir methods" in which a viscous damping applied in an outer region of a MD computational cell has been used to adsorb sound waves and dislocations generated in the process of crack propagation[14] or energetic particle bombardment.[15] An alternative approach is to combine the MD model with the continuum finite element method.[2,3,4,16] The advantage of this approach is the ability to study the long-range propagation of the waves and their interaction with each other and inhomogeneities in the media.[16] For the cases, however, when the aim is merely to avoid artifacts due to pressure wave reflection the above approaches appear to be excessively complex and computationally expensive. In this work we adopt a simple and computational efficient non-reflecting boundary condition based on analytical evaluation of the forces acting at the molecules in the boundary region from the outer "infinite medium".

To understand the origin of the forces acting at the boundary in the setup shown in Fig. 2a, we first consider a larger computational cell, Fig. 3, and plot the pressure development at the depth of the proposed boundary, 100 nm, Fig. 5. In the regime of inertially confined thermoelastic expansion, the pressure profile formed by the end of the laser pulse, Fig. 3, follows the laser energy deposition, $P(z) = \Gamma \Phi / L_p \exp\left[-z/L_p\right]$, where L_p is the laser penetration depth,

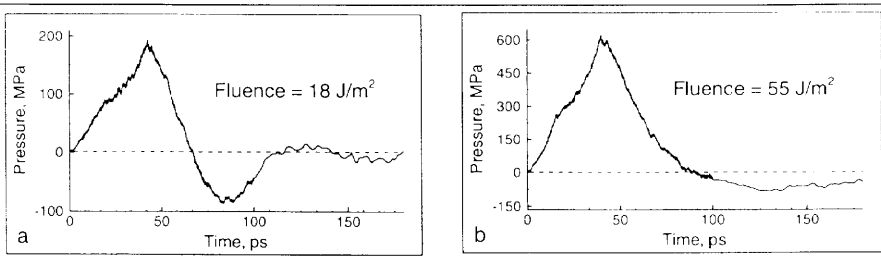

Figure 5. Temporal pressure profiles at 100 nm below the surface for the computational setup shown in Fig. 2a. Laser penetration depth is 50 nm, and pulse width is 15 ps.

Φ is the fluence, and Γ is the Grüneizen coefficient (we neglecting here the temperature dependence of Γ). At the depth of 100 ps this leads to a nearly linear increase of the pressure during the laser pulse, 15 ps, with the final pressure proportional to the laser fluence, Fig. 5. The initial pressure distribution is a source of pressure waves that, due to interaction with the free surface of the sample, form a characteristic bipolar pulse propagating deeper into the sample, Fig. 5a. At laser fluences above the threshold for ablation the tensile phase (negative pressure) is obscured by superposition with the compressive recoil pressure from the ejection of the ablation plume, Fig. 5b.

In our approach the boundary condition is a set of terminating forces F_T that are applied to the atoms in the boundary region. The width of the boundary region is equal to the cut-off distance of the interaction potential used in the MD region. For molecules in the boundary region the parts of the force component in the direction normal to the surface that are due to the interaction with neighbors located closer to the boundary are substituted by terminating forces. In the calculation of the terminating forces that are updated at each integration step, we take into account three effects, namely, the static forces that mimic interaction with molecules beyond the computational cell, F_0, the forces due to the pressure wave propagation through the boundary region, F_W, and the forces due to the direct laser energy absorption in and around the boundary region during the laser pulse, F_L.

The contribution of the pressure wave to the terminating force, F_W, is based on the assumption that the pressure wave propagates as a traveling wave with velocity c. The F_W per molecule then should be proportional to the instantaneous velocity of the boundary, u, as $F_W = S_M Z u$, where $Z=\rho c$ is the acoustic impedance, S_M is the surface area per molecule, and ρ is the density. The force due to the laser energy absorption, F_L, is assumed to rise linearly with time, t, during the laser pulse. In order to account for relaxation of the laser induced pressure we multiply F_L by a damping factor taken in the form proposed in Ref. 17, $D=L_p(1-\exp(tc/L_p))/tc$. As shown in Fig. 6, the resulting terminating force, $F_T(\Phi,t,u)=F_0+F_L(\Phi,t)+F_W(u)$ provides a good approximation of the real forces from the outer part of material obtained from larger scale simulations.

We have used the boundary condition described above in two and three-dimensional simulations with both simulation setups shown in Fig. 2 and were able to completely eliminate simulation artifacts associated with the reflection of the pressure wave from the boundary of the MD computational cell. The boundary condition allows one to restrict area of the MD simulation

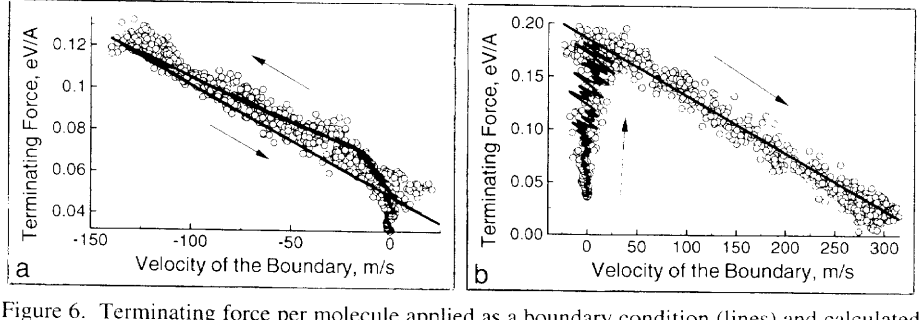

Figure 6. Terminating force per molecule applied as a boundary condition (lines) and calculated directly from a larger scale simulation (data points). The forces for two cases are shown. The laser penetration depth is a) half the depth of the computational cell and b) much longer than the depth of the cell (even energy deposition). Arrows show the direction of time development.

to the region where active processes of laser induced melting, ablation and damage occur. This significantly expands the scope of phenomena that can be addressed and allows to use irradiation parameters comparable to the experimental values.[9] A snapshot from such a large scale simulation is shown in Fig. 7.

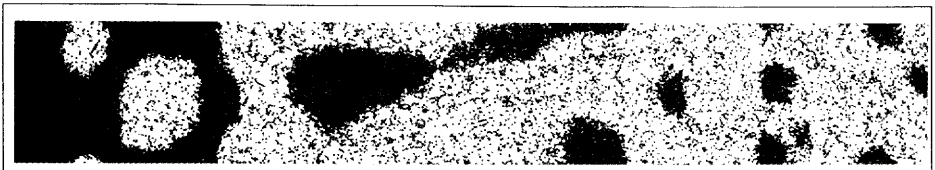

Figure 7. Snapshot from a large-scale three-dimensional molecular dynamics simulation at 400 ps after irradiation with 150 ps laser pulse at a fluence of 55 J/m^2. The laser penetration depth is 50 nm. The initial depth of the computational cell in the direction of incident laser pulse is 100 nm. Non-reflecting boundary condition is applied at the bottom of the computational cell. The simulation is performed with the breathing sphere model.

ACKNOWLEDGMENTS.

This work was supported by NSF and ONR through the MFEL Program. The computational support for this work was provided by the IBM-SUR Program and the Center for Academic Computing at PSU. We thank Victor Sparrow for a stimulating discussion.

REFERENCES

1. F. Cleri, S. R. Phillpot, D. Wolf, and S. Yip, J. Am. Ceram. Soc. **81**, 501 (1998).
2. S. Kohlhoff, P. Gumbsch, and H. F. Fischmeister, Phil. Mag. A **64**, 851 (1991).
3. E. B. Tadmor, M. Ortiz, and R. Phillips, Phil. Mag. A **73**, 1529 (1996).
4. H. Rafii-Tabar, L. Hua, and M. Cross, J. Phys.: Condens. Matter **10**, 2375 (1998).
5. O. Shenderova, D. W. Brenner, A. Nazarov, A. Romanov, and L. Yang, Phys. Rev. B. **57**, R3181 (1998).
6. *Proceedings of the 4th International Conference on Laser Ablation*, edited by R. E. Russo, D. B. Geohegan, R. F. Haglund, Jr., and K. Murakami, Appl. Surf. Sci. **127-129** (1998).
7. L. V. Zhigilei, P. B. S. Kodali, and B. J. Garrison, J. Phys. Chem. B **101**, 2028 (1997); J. Phys. Chem. B **102**, 2845 (1998).
8. L. V. Zhigilei, P. B. S. Kodali, and B. J. Garrison, Chem. Phys. Lett. **276**, 269 (1997).
9. L. V. Zhigilei and B. J. Garrison, Appl. Phys. Lett., in press, 1999.
10. L. V. Zhigilei and B. J. Garrison, Appl. Phys. Lett. **71**, 551, (1997); Rapid Commun. Mass Spectrom., **12**, 1273 (1998).
11. L. V. Zhigilei and B. J. Garrison, Appl. Surf. Sci. **127-129**, 142 (1998); *Laser-Tissue Interaction IX*, edited by S. L. Jacques (SPIE Proceedings Series, Vol. 3254, Washington, 1998), p. 135.
12. D. Kim and C. P. Grigoropoulos, Appl. Surf. Sci. **127-129**, 53 (1998).
13. V. Venugopalan, N. S. Nishioka, and B. B. Mikic, Biophysical Journal. **70**, 2981 (1996).
14. B. L. Holian and R. Ravelo, Phys. Rev. B 51, 11275 (1995).
15. M. Moseler, J. Nordiek, and H. Haberland, Phys. Rev. B **56**, 15439 (1997).
16. J. A. Smirnova, L. V. Zhigilei, and B. J. Garrison, Comput. Phys. Commun., in press, 1999.
17. R. S. Dingus and R. J. Scammon, *Laser-Tissue Interaction IX*, edited by S. L. Jacques (SPIE Proceedings Series, Vol. 1427, Washington, 1991), p.45.